



Published in final edited form as:

Biomaterials. 2012 January ; 33(1): 29–37. doi:10.1016/j.biomaterials.2011.09.044.

Active leukocyte detachment and apoptosis/necrosis on PEG hydrogels and the implication in the host inflammatory response

Heather Waldeck, Ph.D.^a, Xintong Wang, Ph.D.^b, Evan Joyce^a, and Weiyuan John Kao, Ph.D.^{a,c,d}

^aDepartment of Biomedical Engineering, College of Engineering, University of Wisconsin-Madison, WI, USA

^bDepartment of Biomedical Engineering, University of Minnesota, Minneapolis, MN USA

^cSchool of Pharmacy, University of Wisconsin-Madison, WI, USA

^dDepartment of Surgery, University of Wisconsin-Madison, WI, USA

Abstract

Monocytes/Macrophages have long been recognized as key players in inflammation and wound healing and are often employed *in vitro* to gain an understanding of the inflammatory response to biomaterials. Previous work has demonstrated a drastic decrease in primary monocyte adherent density on biomaterial surfaces coupled with a change in monocyte behavior over time. However, the mechanism responsible for this decrease was unclear. In this study, we explored active detachment and cellular death as possible regulating factors. Specifically, extracellular TNF- α and ROS production were analyzed as potential endogenous stimulators of cell death. MMPs, but not calpains, were found to play a key role in active monocyte detachment. Monocyte death was found to peak at 24hr and occur by both apoptosis and necrosis as opposed to polymorphonuclear leukocyte death which mainly occurred through apoptosis. Finally, TNF- α and ROS production were not found to have a causal relationship with monocyte death on TCPS or PEG surfaces. The occurrence of primary monocyte apoptosis/necrosis as well as active detachment from a material surface has implications not only in *in vitro* study, but also in the translation of the *in vitro* inflammatory response of these cells to *in vivo* applications.

Keywords

apoptosis; cell adhesion; cell culture; hydrogel; monocyte

© 2011 Elsevier Ltd. All rights reserved.

^{*}W. John Kao (Corresponding author) School of Pharmacy, University of Wisconsin-Madison, 777 Highland Ave, Madison, WI 53705, USA. Tel: +1 608 263 2998 Fax: +1 608 262 5345 wjkao@pharmacy.wisc.edu.

Heather Waldeck: School of Pharmacy, University of Wisconsin-Madison, 777 Highland Ave, Madison, WI 53705, USA. Tel: +1 608 262 4616 Fax: +1 608 262 5345 hmwaldeck@wisc.edu

Xintong Wang: Biomedical Engineering, University of Minnesota, 312 Church St. SE, Minneapolis, MN 55455, USA. Tel: Fax: wang2571@umn.edu

Evan Joyce: School of Pharmacy, University of Wisconsin-Madison, 777 Highland Ave, Madison, WI 53705, USA. Tel: +1 608 262 4616 Fax: +1 608 262 5345 ejoyce@wisc.edu

Publisher's Disclaimer: This is a PDF file of an unedited manuscript that has been accepted for publication. As a service to our customers we are providing this early version of the manuscript. The manuscript will undergo copyediting, typesetting, and review of the resulting proof before it is published in its final citable form. Please note that during the production process errors may be discovered which could affect the content, and all legal disclaimers that apply to the journal pertain.

Introduction

Monocytes/Macrophages have long been recognized as key players in inflammation and wound healing [1–3]. Along with polymorphonuclear leukocytes (PMNs), these phagocytes are among the first responders to a site of injury where they act to clear away debris and defend against bacterial infiltration [3, 4]. Critical to these functions is the ability of these cell types to produce high levels of reactive oxygen species in what is known as a “respiratory burst” which can act to degrade foreign particles and/or mediate cellular signaling [5–7]. Additionally, both PMNs and macrophages produce a milieu of other chemical mediators which can influence the progression of subsequent healing events [4, 8]. The differential maturation of monocytes into a particular macrophage phenotype also allows infiltrating blood monocytes to play multiple roles in the host response [9, 10]. Biomaterials research often aims to understand and modulate the host response in order to affect a more favorable and/or efficient end-stage healing result. To this end, *in vitro* investigation of macrophage response to biomaterials has been approached through a variety of methodologies. For example, as opposed to using cancerous human and murine cell lines which have phenotypes similar to monocyte/macrophage (*e.g.* U937, THP-1, RAW264.7), primary monocytes can be isolated from whole blood and immediately seeded onto a biomaterial surface to examine the resulting inflammatory response [11–13]. Alternatively, these same primary monocytes can be allowed to differentiate into a more macrophage phenotype by culturing on tissue culture polystyrene (TCPS) surfaces for extended time periods with or without exogenous stimulation [14–16]. In either case, the microenvironment created by the culture conditions has been shown to play a direct role in determining the subsequent response of these primary cells [17–19].

Previous work has begun to explore the influence of culture conditions on the behavior of primary monocytes *in vitro*. For example, differences were observed in adherent density and cytokine release profiles of primary human monocytes exposed to TCPS and poly(ethylene glycol) (PEG) hydrogel surfaces cultured in either fetal bovine serum (FBS) or autologous human serum (AHS) [12]. The effect of serum source was most evident in the observed 3- and 10-fold increase in adherent cell density on TCPS and PEG hydrogel surfaces, respectively, when AHS versus FBS was employed. In addition to the impact of exogenous factors to the culture system, the introduction of the *in vitro* environment itself can impact the response of primary cells. On a variety of substrates *in vitro*, a drastic decrease in primary monocyte adherent density has been consistently observed over a one week period with a particularly significant drop after 24 hours [11–13, 19–24]. Additionally, this decrease in adherent density is usually accompanied by a temporal alteration in cell behavior (*e.g.* cytokine or growth factor release) [11, 12, 21–24]. The mechanism regulating the decrease in monocyte adherent density on these substrates and its possible impact on cell behavior, however, remains unclear. Several possible explanations exist including either an active process of cell detachment or a loss of cell viability upon contact with the substrates *in vitro*.

Possible active detachment of monocytes may be mediated by a decrease in adhesion strength related to, for example, increased cell migration or a cytoprotective affect stimulated by interaction with the biomaterial substrates. Matrix metalloproteinases (MMPs) and calpains have been repeatedly shown to play significant roles in cell migration and invasion by regulating integrin function [25–28]. As a type of intracellular protease, the calpains contribute to cell migration by interacting and cleaving a broad range of integrins and cytoskeleton proteins, *e.g.*, β integrins, β -catenin, cadherins, filamin, talin 1 and vinculin [29–36]. The MMPs are a large family of extracellular proteases which are able to cleave cytokines and extracellular matrix proteins to promote cell proliferation, migration and differentiation [37]. Alternatively, decreased monocyte density on these biomaterial

substrates may be due to an increase in the occurrence of cell death leading to a loss of cell density on the surface. Of particular interest for biomaterial research is the mechanism by which the cells are possibly dying. For example, apoptosis, or programmed cell death, is widely considered anti-inflammatory. In contrast, necrosis and/or necroptosis, often releases signaling molecules, such as DNA or high mobility group box protein 1, which can trigger an inflammatory response [38, 39]. There are several potential endogenous effectors that could be responsible for a loss of cell viability. For example, TNF- α has been shown to trigger both apoptosis and necroptosis through binding to the death receptor, TNFR1 [40, 41]. An elevated TNF- α level is crucial in the inflammatory response and monocytes are the main source of TNF- α in wounds [42–44]. Thereby, auto- and paracrine signaling by this cytokine may contribute to an increase in cell death. Alternatively, ROS has been shown to facilitate cell death by both damaging cells and mediating signaling cascades by altering cell redox states, chemically modifying critical proteins, or acting as a secondary messenger [41, 45–48]. Therefore, an increase in the production of extracellular ROS by phagocytes *in vitro*, leading to a highly oxidative microenvironment similar to what is seen in chronic wounds, may contribute to an increase in cell death. In this study, we explored active monocyte detachment via MMPs or calpains and cellular death as explanations for decreased monocytes density *in vitro* over time on TCPS and PEG hydrogel surfaces. TCPS was selected because it is a commonly used reference material and PEG hydrogels were selected because they have been shown to limit protein adsorption while supporting monocyte adhesion while having differing properties than TCPS [12, 13]. Additionally, extracellular TNF- α and ROS production were analyzed for a potential causal relationship with monocyte or PMN death.

Materials and Methods

PEGdA and PEG hydrogel synthesis

Poly(ethylene glycol) diacrylate (PEGdA) was prepared using a modified protocol which has been previously described [49]. Briefly, PEG diol (3.4kDa; Sigma Aldrich, St. Louis, MO) was reacted with acryloyl chloride (Sigma Aldrich) in the presence of triethylamine (TEA; Sigma Aldrich) in a 1:8:8 molar ratio overnight at room temperature in the dark. The resulting acrylated PEG was then purified by dissolving in dichloromethane and precipitating in cold diethyl ether. The degree of acrylation was determined to be >95% using $^1\text{H-NMR}$ and high performance liquid chromatography. The PEG hydrogels were prepared by dissolving 10 or 15 wt% PEGdA and the photoinitiator, 1 wt% Irgacure 2959 (Ciba), in ddH₂O. The solution was poured into Teflon molds and cured with UV CF1000 LED ($\lambda_{\text{max}} = 365\text{nm}$, Clearstone Technologies). The PEG hydrogels were sterilized with 70% ethanol for 45 min and then washed five times with phosphate buffered saline (PBS, pH 7.4) over 60min to remove ethanol, unreacted PEGdA, and Irgacure 2959. Immediately prior to the addition of cells, the hydrogels were equilibrated in RPMI 1640 (Gibco, Invitrogen, Carlsbad, CA) for 2hr at 37°C and 5% CO₂.

Primary monocyte and PMN isolation

Primary monocytes and PMNs were isolated using a density gradient based methodologies modified from previously published work [50]. Briefly, 60 mL citrated whole blood was collected from more than one healthy adult volunteer. The whole blood was diluted in Dulbecco's phosphate buffered saline (DPBS; Hyclone, Thermo Scientific) supplemented with 1mM EDTA (Fisher Scientific) and underlayered with Ficoll-Paque Premium ($\rho=0.077$; GE Healthcare, Pittsburgh, PA). After centrifugation at 400 $\times g$ for 30min at room temperature (RT), mononuclear cells were separated from granulocytes and erythrocytes. The mononuclear cells were then separated using a Percoll gradient and the resulting band of monocytes was collected. This isolation procedure resulted in ~80–90% monocyte purity

based on flow cytometry analysis (data not shown) with the primary contaminant being lymphocytes. The initial separation of granulocytes from erythrocytes was done using a 2% dextrose gradient at RT. The remaining erythrocytes were lysed using several incubations with cold ddH₂O. All steps besides the density gradient separations were done on ice or at 4°C to minimize PMN activation. While a majority of the isolated granulocytes are PMNs, a small percentage (<1%) of contamination by basophils and eosinophils is possible. The isolated monocytes and PMNs were re-suspended in cold RPMI 1640 (Gibco, Invitrogen) and the cell concentration was calculated using a hemocytometer. Typically, 12–20×10⁶ monocytes and 80–100×10⁶ PMNs were isolated from 60 mL whole blood. Cells were statically seeded on PEG hydrogels fit into 48- or 96-well cell culture plates or the TCPS (Costar®, Corning Inc., Corning, NY) surface directly at a concentration of 10⁶ cells/mL (6.6×10⁴ and 6.3×10⁴ cells/cm² for 48- and 96- well plates, respectively) suspended in RPMI 1640 media with 10% autologous human serum at 37°C and 5% CO₂. All fluorescence-based assays were performed on cultures containing RPMI 1640 without phenol red to prevent interference with the fluorescent signal.

Effects of protease inhibitors on monocyte adhesion

The MMP inhibitor GM6001 (Calbiochem, EMD Chemicals, Darmstadt, Germany) and the calpain inhibitor PD150606 (Sigma) were used to study the effects of MMPs and calpains on monocyte adhesion [51, 52]. Optimization of concentrations of the inhibitors to be employed in future studies was performed by adding gradient concentrations of GM6001 (5, 10, 25 and 50μM) and PD150606 (10, 50, 100 and 200μM) to monocyte culture media. The supernatant was removed after incubating for 2hr and the adherent cells were then washed twice with RPMI 1640. Adherent cells were imaged with a digital camera attached to inverted microscope (Nikon Eclipse TE 300). The cell number on each image (sampling area: 2.385mm²/image) was counted to determine cell density per mm². The experiment was repeated three times independently and three images were taken for each substrate at each time point. The number of adherent cells increased with the increase of PD150606 concentration from 0 to 50μM and then decreased from 50 to 200μM (Figure 1A). The number of adherent cells also increased with the concentration of GM6001 from 0 to 5μM, and then decreased from 5 to 50 μM (Figure 1B). The monocyte adhesion on TCPS with PD150606 and GM6001 generally showed the same decreasing trend after incubation from 1 to 24hr and the number of adherent cells dropped significantly at 24hr for both PD150606 and GM6001, suggesting these inhibitors were probably exhausted after long incubation (data not shown). Based on the results of these studies, the incubation time and the concentrations of GM6001 and PD150606 were optimized to enable the highest number of adherent cells for the following study. Monocytes were seeded on TCPS plates with or without PEG hydrogel. 10μM GM6001 or 50μM PD150606 was added to the culture medium and the cells were incubated with the inhibitors for 2hr before each time point. The adherent cells were then washed twice with DPBS, imaged, and counted at 2, 24, 96 and 168hr as described above. To further ascertain the viability of monocytes detached from different substrates, cell culture supernatants were collected and transferred into a black TCPS plate at 2, 24, 96 and 168 hours. The amount of live and dead cells were measured simultaneously via a fluorescent assay (MultiTox-Fluor™, Promega, Madison, WI) at 400_{ex}/505_{em} and 485_{ex}/520_{em} respectively according to the manufacturer's instruction.

Determination of TNF-α release

Cells were seeded into a 48-well TCPS plate with or without PEG hydrogels in RPMI 1640 supplemented with 10% pooled human sera (Sigma). At 2, 24, 96 and 168hr, supernatant was collected from each well and ELISA assays were performed to determine the concentrations of TNF-α (Invitrogen). Cell culture supernatants without cells served as controls. A standard curve was created for TNF-α ($y = -0.3117x^2 + 0.719x + 0.0024$, $r^2 = 0.999$),

where x is adsorbed/absorbed protein ($\mu\text{g}/\text{cm}^2$) and y is the absorbance value. The protein concentration in the supernatant was then calculated by comparing the absorbance value to the standard curve.

The effect of TNF- α on cell adhesion

Various concentrations of recombinant human TNF- α (R&D Systems, Minneapolis, MN) were employed to determine its effect on monocyte adhesion to TCPS. Human primary monocytes were isolated and seeded on TCPS (5×10^4 cells/well) in media supplemented with 0.01, 0.05, 0.5, 5 or 50 ng/mL TNF- α . Medium without TNF- α served as control. The supernatants were removed at 2 and 12 hr and adherent cells were quantified using microscopic imaging as described above.

Determination of extracellular ROS production

At 2, 24, and 96 hr, supernatant from monocyte or PMN cultures was removed and OxyBURST Green H₂HFF BSA (10 $\mu\text{g}/\text{ml}$; Invitrogen) in Hank's buffered saline solution (Gibco[®] Invitrogen) with or without 100 nM phorbol 12-myristate 13-acetate (PMA; Sigma) was added to the wells containing cells adhered to TCPS or PEG hydrogel surfaces. OxyBURST Green H₂HFF BSA contains a fluorescein derivative conjugated to bovine serum albumin (BSA) which fluoresces upon oxidation by ROS. A review of the literature and comparison of the chemistry to other probes suggests that this probe can be oxidized by a variety of reactive oxygen species, but not reactive nitrogen species, including both more stable and unstable species. PMA is a known stimulator of protein kinase C which activates NADPH oxidase 2, the main source of ROS in monocytes and PMNs. The fluorescence was then monitored (485_{ex}/520_{em}; Fluorstar Optima, BMG Labtech, Cary, NC) over 2 hr at 37°C. The mean fluorescence intensity (MFI) after 2 hr was compared to a fluorescein standard curve (1, 5, 10, 25, 50 nM) to allow for plate-to-plate comparisons. All data is presented as the equivalent (eq.) fluorescein MFI. As the probe was present while the cell was in contact with a biomaterial surface for an extended period of time, oxidation by both stable and unstable ROS is possible.

Determination of viability, apoptosis, necrosis, and secondary necrosis

The level of monocyte and PMN viability, apoptosis, and necrosis at 2, 24, 48, 96, and 168 hr was determined using the ApoTox-Glo kit (Promega). Briefly, viability was assessed by measuring the ability of cells with intact membranes to cleave a fluorogenic, cell-permeant, peptide substrate, glycyphenylalanyl-aminofluorocoumarin (400_{ex}/505_{em}). The resulting fluorescent signal is proportional to the number of living cells. Primary and secondary necrosis was assessed by measuring the cleavage of fluorogenic, cell-impermeant, peptide substrate, bis-alanylalanyl-phenylalanyl-rhodamine 110 (485_{ex}/520_{em}) by a "dead-cell protease" which is released from cells with permeable membranes. A luminogenic caspase-3/7 substrate, which contains the tetrapeptide sequence DEVD, was used to measure the activity of both caspase 3 and 7. The activation of both caspases is downstream of the intrinsic and extrinsic apoptotic pathways. Secondary necrosis was assessed by measuring the activity of caspase-3 in the supernatant [53]. 70 μl of supernatant from monocyte and PMN cultures was diluted in 130 μl buffer (20 mM HEPES, 10% glycerol, 2 mM DTT) and the fluorogenic peptide substrate Ac-DEVD-AMC was added to a final concentration of 20 μM . The solution was incubated at 37°C for 2 hr and then the mean fluorescence intensity (MFI) of the free-AMC was assessed (380_{ex}/460_{em}). Supernatant from a no-cell condition served as a negative control.

Additionally, apoptosis and necrosis were qualitatively observed using fluorescence microscopy. Briefly, at 2, 24, 48, 96, and 168 hr, monocytes and PMNs were rinsed with cold DPBS (Mediatech Inc., Manassas, VA) and fluorescent dyes were added according to

the manufacturer's protocol adapted for a 96-well plate format (Vybrant Apoptosis Assay Kit #6; Invitrogen). Apoptosis detection was based on the translocation of phosphatidylserine from the inner to outer membrane of the plasma membrane in apoptotic cells. The high affinity of Annexin V for phosphatidylserine was used to associate a fluorescent molecule (Alexa-Fluor 350; 365_{ex}/440_{em}) to the membrane of apoptotic cells. Primary and secondary necrosis was detected using the nucleic acid-binding propidium iodide dye (488_{ex}/575_{em}) which cannot penetrate the membranes of live or early apoptotic cells. Live cells demonstrated no or a very low level of fluorescence.

Statistical analysis

All data is presented as the mean \pm standard deviation of samples in independent experiments ($n \geq 3$) and were analyzed by ANOVA or student's t-test where values of $p < 0.05$ were considered statistically significant.

Results

MMP-mediated active detachment of monocytes

Our previous studies found that the number of adherent monocytes on both PEG hydrogel and TCPS decreased with time, with a dramatic decrease in adhesion occurring between 24 and 96hr [12, 13]. These results were also replicated in this study with non-treated monocytes (Figure 2). Correlating with these results, both viable and non-viable non-adherent monocyte density peaked at 96hr (Figure 3A) suggesting that in addition to cell death, active detachment may play a role in the decrease in adherent density. In this study, inhibitors to MMPs (GM6001) and calpains (PD150606) were employed to determine the effect of these proteases on monocyte adhesion since they have been repeatedly shown to play significant roles in cell migration and invasion [25–28]. After treatment with GM6001, adherent monocyte density on TCPS was enhanced ($p < 0.05$; Figure 2) and non-adherent monocyte density on both PEG and TCPS surfaces decreased (Figure 3B) significantly over time. Conversely, inhibition of calpains only led to an increase in adherent monocyte density on TCPS at 2hr ($p < 0.01$; Figure 2) and did not significantly alter the number of non-adherent monocytes (Figure 3C) which suggests that the effect of calpains is less important than the effect of MMPs in modulating cell adherent density. However, adherent monocyte density on PEG hydrogels after treatment with PD15606 at 2 and 24hr, though not significant, was generally higher than with non-treated conditions. The high amount of non-viable non-adherent monocytes (Figure 3A), however, suggests that cellular death is still a major factor in the decrease in adherent cell density on both TCPS and PEG surfaces over time.

Leukocyte death as mediated by extracellular TNF- α and ROS

In order to examine possible endogenous causes for cell death *in vitro* on TCPS and PEG hydrogel surfaces, the levels of two known effectors of cell death that are produced by monocytes were examined: TNF- α and ROS. The TNF- α concentration in cell culture supernatant increased from 2 to 24hr followed by a significant decrease from 24 to 168hr when monocytes were cultured on both PEG hydrogel and TCPS (Figure 4). The presence of PEG hydrogels significantly increased the TNF- α concentration at 24 and 96 hours despite the number of adherent monocytes on PEG hydrogels being markedly lower than on TCPS at these time points (Figure 2; [13]). Interestingly, the addition of exogenous TNF- α significantly increased the number of adherent monocytes on TCPS surfaces, though the adherent cell number generally decreased with the higher concentrations of TNF- α (Figure 5).

Both PMNs and monocytes/macrophages are capable of producing high amounts of ROS as a mechanism to degrade foreign entities. Extracellular ROS production by monocytes was analyzed by using a cell membrane impermeable probe which fluoresces upon oxidation. Results using monocytes were compared to PMNs isolated from the same human donor to limit effects of donor variation, as PMNs are a known producer of extracellular ROS *in vitro*. PMNs produced much higher levels of extracellular ROS than monocytes over time with or without PMA stimulation (Figure 6). Moreover, the only significant production of ROS by monocytes without PMA stimulation was seen at 2hr (Figure 6A) and upon seeding (data not shown). PMN production of ROS on both PEG and TCPS surfaces demonstrated no change or a decrease from 2 to 24hr followed by an increase in production at 96hr (Figure 6B). Finally, monocyte cultured for 9 days on TCPS produced marginal extracellular ROS even with PMA stimulation (<1nM equivalent fluorescein MFI).

Apoptosis and necrosis of leukocytes

In order to better understand the type of cell death occurring *in vitro* on PEG and TCPS surfaces, monocytes and PMN viability, apoptosis, and necrosis were analyzed simultaneously using fluorescent and luminescent probes. Similar to the results of previous microscopic assays (Figure 2; [12, 13]), monocyte and PMN viability decreased significantly after 24hr ($p<0.05$; Figure 7). Additionally, apoptosis and necrosis peaked at 24hr for both cell types on TCPS and PEG surfaces. The activity of necrosis indicators were also elevated at 168hr for monocytes. Higher activity of necrosis indicators was present with monocytes in the presence of TCPS at 24hr as compared to PEG surfaces ($p<0.05$; Figure 7A). In the case of PMNs, higher levels of caspase 3/7 activity was seen with PEG compared to TCPS at 2hr; however, at 24hr, higher caspase 3/7 activity was seen with TCPS surfaces ($p<0.05$; Figure 7B). As the assay used to determine the incidence of necrosis did not discriminate between primary and secondary necrosis, the activity of caspase-3 in the supernatant was assayed to determine the level of secondary necrosis. Evidence of PMN secondary necrosis peaked at 24hr on both surfaces and decreased over time (Figure 8). No significant evidence of monocyte secondary necrosis was seen over time except on PEG surfaces at 168hr. Qualitatively, microscopic fluorescence imaging of monocytes and PMNs adhered to both PEG and TCPS surfaces demonstrated instances of both the translocation of phosphatidylserine from the inner to outer membrane of the plasma membrane as well as the staining of nuclear DNA by the cell-impermeable dye, propidium iodide, at 2, 24, 48, 96, and 168hr (Figure 9). Thus, both types of assays demonstrated the occurrence of both apoptosis and necrosis by monocytes and PMNs. However, while the necrosis observed for PMNs may be primarily due to secondary necrosis after 2hr, monocytes seem to be undergoing primary necrosis *in vitro*.

Discussion

Previous work has demonstrated a decrease in primary human monocyte adherent density on biomaterial surfaces *in vitro* over time often accompanied by time-dependent alterations in cell behavior [11–13, 19–24]. In this study, we found that monocytes are removed from these substrates through both active detachment mechanisms and monocyte death by both apoptosis and necrosis. MMPs, but not calpains, appeared to play a critical role in the detachment of monocytes from TCPS and PEG surfaces as shown by an increase in adherent cell density (TCPS; Figure 2A) and a decrease in non-adherent cell density (TCPS and PEG; Figure 3) after treatment by an MMP inhibitor. The lack of an increase in adherent density on PEG hydrogel surfaces after treatment with GM6001 and the greater impact of PD150606 on adherence to PEG surfaces (Figure 2B), however, indicates that the regulating mechanism of cell adhesion on TCPS and PEG hydrogel may be different. Calpains primarily play a role in the destabilization or disassembly of adhesion complexes. PD150606

can thereby act to increase cell adhesion by reducing the dissociation of integrins from the cytoskeleton through calpain activity [54]. Thus, integrin cleavage by calpains may affect initial monocyte adhesion to TCPS; however, it does not appear to play a major role in the monocyte interaction with the surface at later time periods. Although not found to cause a significant increase in adherent density, calpains may also play a larger role in monocyte detachment to PEG hydrogels (Figure 2B). In contrast, the mechanism of action of GM6001 on cell adhesion through inhibition of MMPs is largely unknown. MMPs modulate cell behavior through multiple mechanisms such as cleaving either the extracellular proteins to which cells bind or cytokines which can control downstream adhesive events. Additionally, MMPs often bind to integrin receptors such as $\alpha_v\beta_3$, $\alpha_2\beta_1$ and $\alpha_3\beta_1$, in order to efficiently cleave extracellular proteins [55–57]. The close interaction between MMPs and integrins, however, may lead to the cleavage of integrins from the cell membrane. Recent reports have shown that MMP-9 can lead to the cleavage of the β_2 integrin subunit from macrophages and the β_1 integrin from endothelial cells [58, 59]. Thus, inhibition of MMPs may reduce the occurrence of multiple events which can lead to a decrease in monocyte adherent density. For example, on both PEG hydrogels and TCPS, GM6001 treated monocytes showed significantly enhanced cell viability than the other groups, especially at later time points (96 and 168hr, $p < 0.01$; Figure 3). This observation is in agreement with a previous report that showed the inhibition of MMPs by GM6001 protects cells from lethal toxin-mediated cell death [60]. Alternatively, although not examined in this study, alterations in monocyte adhesion strength to these surfaces could also be altered over time and through treatment with GM6001. Thereby, events inherent to *in vitro* culture, such as media changes, may have less impact on removing weakly adherent cells from the surface.

The production of TNF- α and ROS, two possible effectors of cell death, did not positively correspond to apoptotic or necrotic cell death. The addition of exogenous TNF- α led to an increase in the number of viable adherent monocytes, however, the density generally decreased with increasing TNF- α concentrations (Figure 5). Based on this result and the overall low concentration of TNF- α released by monocytes in the presence of TCPS and PEG hydrogels (generally less than 1 ng/ml; Figure 4), it is unlikely that this amount of TNF- α was sufficient to lead to high levels of programmed cell death. Additionally, TNF- α interaction with TNFR1 has also been shown to lead to multiple downstream outcomes including enhanced survival [40]. Although monocytes/macrophages are considered one of the primary causes of a highly oxidative wound microenvironment through the release of ROS, within the conditions of this study, monocytes only produced a small amount of extracellular ROS at 2hr in response to both TCPS and PEG surfaces (Figure 6A). Furthermore, this slight amount of production at the earliest time point may have only been an artifact from the isolation procedures as no differences were seen between surfaces. Therefore, extracellular ROS production is unlikely to be a primary mechanism of monocyte death on these substrates. Even though intracellular and extracellular ROS are commonly associated with mechanisms of cell death, ROS and reactive nitrogen species have also been shown to play critical roles in mediating fibroblast adhesion [61] and monocyte survival [45, 62]. As such, the role of extracellular ROS in *in vitro* primary monocyte culture may possibly have multiple consequences. In contrast to monocytes, PMN extracellular ROS production, similarly high at 2hr, also demonstrated enhanced ROS levels at 96hr despite a drastic decrease in cell viability (Figure 6B). In this case, ROS production in concurrence with cell death may provide a possible explanation for this observation. Previous research has determined that ROS play a key role in the spontaneous apoptosis of PMNs [47]. The later production of ROS may also be related to the ability of PMNs to undergo an alternative mechanism of cell death, termed “ETosis”, which results in the production of “extracellular traps” which consist of net-like structures comprised primarily of DNA. It has been shown that high levels of ROS are required for ETosis to occur; in fact, PMA is often used to trigger ETosis [63]. Although the occurrence of ETosis is typically associated with an

antibacterial strategy, some evidence exists for stimulation by biomaterials [64]. In this study, qualitative observations of ETosis based on cell morphology was observed on both TCPS and PEG hydrogel surfaces in the form of DNA-based extracellular structures similarly to those seen in published literature (data not shown). Alternatively, monocyte detachment mediated by MMPs, as described previously, may also lead to an increase in monocyte death over time. The lack of an extended microenvironment within the *in vitro* culture system may alter the effect of detachment on monocyte/PMN viability compared to what is observed during wound remodeling *in vivo*. While approximately one third or greater of the non-adherent monocytes were viable over all time points (Figure 3A), the non-adherent monocytes may be dying at a higher rate than those adhered onto a substrate.

The occurrence and method of cell death in primary cultures is likely an influential factor in the evaluation of the inflammatory response of primary cells *in vitro* and the translation of these observations *in vivo*. In this study, monocyte death, particularly in the first 24hr, occurs by both apoptotic and necrotic mechanisms. This result is consistent with previous work in our lab that found increased levels of high mobility group box protein 1 and growth-related oncogene 2 [12] in monocyte cultures indicative of necrotic cell death. In contrast, evidence of secondary necrosis in PMN cultures indicates that the primary mode of PMN death was likely apoptosis which is consistent with previous literature demonstrating that primary PMNs undergo spontaneous apoptosis upon introduction to *in vitro* culture [47, 65]. Apoptotic and necrotic cell remains can trigger different cellular responses, particularly with phagocytes which are responsible for clearing cell debris. For example, phagocytosis of necrotic cell remains by macrophages is thought to trigger differentiation to a more inflammatory phenotype while apoptotic remains have been shown to cause a wound healing phenotype [66, 67]. Therefore, the manner in which cells are dying *in vitro* may lead to an inflammatory response not likely to be observed *in vivo*. In particular, as seen with PMNs, without the proper clearance mechanisms, apoptotic bodies will undergo secondary necrosis thus altering the inflammatory response of the remaining viable cells.

Conclusion

The mechanisms leading to a decreased adherent density of primary human monocytes on TCPS and PEG hydrogel surfaces was partially elucidated. MMPs, but not calpains, were found to play a key role in the active detachment of monocytes from these substrates. Monocyte death through both apoptosis and necrosis was also found to be a cause for the decrease in monocyte adherent density. TNF- α release by monocytes peaked at 24hr, however, differences in production when exposed to TCPS versus PEG surfaces were not reflected in changes to cell viability so a causal relationship could not be established. Similarly, ROS production by monocytes was seen only at 2hr and therefore is not a sole endogenous cause of cell death. The occurrence of primary monocyte apoptosis/necrosis as well as active detachment from a material surface has implications not only in *in vitro* study, but also in the translation of the *in vitro* inflammatory response of these cells to *in vivo* applications.

Acknowledgments

The authors would like to thank David Cantu for his assistance with phlebotomy procedures. This work was supported by NIH Grant R01 EB6613.

References

1. Lucas T, Waisman A, Ranjan R, Roes J, Krieg T, Muller W, et al. Differential roles of macrophages in diverse phases of skin repair. *J Immunol.* 2010; 184:3964–3977. [PubMed: 20176743]

2. Eming SA, Krieg T, Davidson JM. Inflammation in wound repair: molecular and cellular mechanisms. *J Invest Dermatol.* 2007; 127:514–525. [PubMed: 17299434]
3. Anderson, JM. Inflammation, wound healing, and the foreign-body response. In: Ratner, BD.; Hoffman, AS.; Schhoen, FJ.; Lemons, JE., editors. *Biomaterials Science: An introduction to materials in medicine.* 2nd ed.. Amsterdam; Boston: Elsevier Academic Press; 2004. p. 296-304.
4. Soehnlein O, Lindbom L. Phagocyte partnership during the onset and resolution of inflammation. *Nat Rev Immunol.* 2010; 10:427–39. [PubMed: 20498669]
5. Thannickal VJ, Fanburg BL. Reactive oxygen species in cell signaling. *Am J Physiol Lung Cell Mol Physiol.* 2000; 279:L1005–L1028. [PubMed: 11076791]
6. Cape JL, Hurst JK. The role of nitrite ion in phagocyte function--perspectives and puzzles. *Arch Biochem Biophys.* 2009; 484:190–196. [PubMed: 19402211]
7. Brown DI, Griendling KK. Nox proteins in signal transduction. *Free Radic Biol Med.* 2009; 47:1239–1253. [PubMed: 19628035]
8. Gurtner GC, Werner S, Barrandon Y, Longaker MT. Wound repair and regeneration. *Nature.* 2008; 453:314–321. [PubMed: 18480812]
9. Gordon S, Taylor PR. Monocyte and macrophage heterogeneity. *Nat Rev Immunol.* 2005; 5:953–964. [PubMed: 16322748]
10. Martinez FO, Sica A, Mantovani A, Locati M. Macrophage activation and polarization. *Front Biosci.* 2008; 13:453–461. [PubMed: 17981560]
11. Chung AS, Waldeck H, Schmidt DR, Kao WJ. Monocyte inflammatory and matrix remodeling response modulated by grafted ECM-derived ligand concentration. *J Biomed Mater Res A.* 2009; 91:742–752. [PubMed: 19051303]
12. Schmidt D, Joyce EJ, Kao WJ. Fetal bovine serum xenoproteins modulate human monocyte adhesion and protein release on biomaterials in vitro. *Acta Biomater.* 2011; 7:515–525. [PubMed: 20837169]
13. Wang X, Schmidt DR, Joyce EJ, Kao WJ. Application of MS-based proteomics to study serum protein adsorption/absorption and complement C3 activation on poly(ethylene glycol) hydrogels. *J Biomater Sci Polym Ed.* 2010 June 30. [Epub ahead of print].
14. Labow RS, Meek E, Santerre JP. Hydrolytic degradation of poly(carbonate)-urethanes by monocyte-derived macrophages. *Biomaterials.* 2001; 22:3025–3033. [PubMed: 11575477]
15. McNally AK, Anderson JM. Interleukin-4 induces foreign body giant cells from human monocytes/macrophages. Differential lymphokine regulation of macrophage fusion leads to morphological variants of multinucleated giant cells. *Am J Pathol.* 1995; 147:1487–1499. [PubMed: 7485411]
16. Gantner F, Kupferschmidt R, Schudt C, Wendel A, Hatzelmann A. In vitro differentiation of human monocytes to macrophages: change of PDE profile and its relationship to suppression of tumour necrosis factor-alpha release by PDE inhibitors. *Br J Pharmacol.* 1997; 121:221–231. [PubMed: 9154331]
17. McBane JE, Matheson LA, Sharifpoor S, Santerre JP, Labow RS. Effect of polyurethane chemistry and protein coating on monocyte differentiation towards a wound healing phenotype macrophage. *Biomaterials.* 2009; 30:5497–5504. [PubMed: 19635633]
18. Shi C, Simon DI. Integrin signals, transcription factors, and monocyte differentiation. *Trends Cardiovasc Med.* 2006; 16:146–152. [PubMed: 16781947]
19. Collier TO, Anderson JM. Protein and surface effects on monocyte and macrophage adhesion, maturation, and survival. *J Biomed Mater Res.* 2002; 60:487–496. [PubMed: 11920674]
20. Franklin JP, Stahl GF, Daniels JC. Reversible attachment of human peripheral blood monocytes during in vitro culture. *Immunol Commun.* 1982; 11:477–489. [PubMed: 7169226]
21. Jones JA, Dadsetan M, Collier TO, Ebert M, Stokes KS, Ward RS, et al. Macrophage behavior on surface-modified polyurethanes. *J Biomater Sci Polym Ed.* 2004; 15:567–584. [PubMed: 15264659]
22. Lynn AD, Kyriakides TR, Bryant SJ. Characterization of the in vitro macrophage response and in vivo host response to poly(ethylene glycol)-based hydrogels. *J Biomed Mater Res A.* 2010; 93:941–953. [PubMed: 19708075]

23. Chung A, Gao Q, Kao WJ. Macrophage matrix metalloproteinase-2/-9 gene and protein expression following adhesion to ECM-derived multifunctional matrices via integrin complexation. *Biomaterials*. 2007; 28:285–298. [PubMed: 16979234]
24. Chung AS, Kao WJ. Fibroblasts regulate monocyte response to ECM-derived matrix: the effects on monocyte adhesion and the production of inflammatory, matrix remodeling, and growth factor proteins. *J Biomed Mater Res A*. 2009; 89:841–853. [PubMed: 19437738]
25. Newby AC. Matrix metalloproteinases regulate migration, proliferation, and death of vascular smooth muscle cells by degrading matrix and non-matrix substrates. *Cardiovasc Res*. 2006; 69:614–624. [PubMed: 16266693]
26. Stefanidakis M, Koivunen E. Cell-surface association between matrix metalloproteinases and integrins: role of the complexes in leukocyte migration and cancer progression. *Blood*. 2006; 108:1441–1450. [PubMed: 16609063]
27. Chen P, Parks WC. Role of matrix metalloproteinases in epithelial migration. *J Cell Biochem*. 2009; 108:1233–1243. [PubMed: 19798678]
28. Franco SJ, Huttenlocher A. Regulating cell migration: calpains make the cut. *J Cell Sci*. 2005; 118:3829–3838. [PubMed: 16129881]
29. Pfaff M, Du X, Ginsberg MH. Calpain cleavage of integrin beta cytoplasmic domains. *FEBS Lett*. 1999; 460:17–22. [PubMed: 10571053]
30. Serrano K, Devine DV. Vinculin is proteolyzed by calpain during platelet aggregation: 95 kDa cleavage fragment associates with the platelet cytoskeleton. *Cell Motil Cytoskeleton*. 2004; 58:242–252. [PubMed: 15236355]
31. Rios-Doria J, Day KC, Kuefer R, Rashid MG, Chinnaiyan AM, Rubin MA, et al. The role of calpain in the proteolytic cleavage of E-cadherin in prostate and mammary epithelial cells. *J Biol Chem*. 2003; 278:1372–1379. [PubMed: 12393869]
32. Rios-Doria J, Kuefer R, Ethier SP, Day ML. Cleavage of beta-catenin by calpain in prostate and mammary tumor cells. *Cancer Res*. 2004; 64:7237–7240. [PubMed: 15492240]
33. Franco S, Perrin B, Huttenlocher A. Isoform specific function of calpain 2 in regulating membrane protrusion. *Exp Cell Res*. 2004; 299:179–187. [PubMed: 15302585]
34. Huff-Lonergan E, Mitsuhashi T, Beekman DD, Parrish FC Jr, Olson DG, Robson RM. Proteolysis of specific muscle structural proteins by mu-calpain at low pH and temperature is similar to degradation in postmortem bovine muscle. *J Anim Sci*. 1996; 74:993–1008. [PubMed: 8726731]
35. Carragher NO, Levkau B, Ross R, Raines EW. Degraded collagen fragments promote rapid disassembly of smooth muscle focal adhesions that correlates with cleavage of pp125(FAK), paxillin, and talin. *J Cell Biol*. 1999; 147:619–630. [PubMed: 10545505]
36. Du X, Saido TC, Tsubuki S, Indig FE, Williams MJ, Ginsberg MH. Calpain cleavage of the cytoplasmic domain of the integrin beta 3 subunit. *J Biol Chem*. 1995; 270:26146–26151. [PubMed: 7592818]
37. Manso AM, Elsharif L, Kang SM, Ross RS. Integrins, membrane-type matrix metalloproteinases and ADAMs: potential implications for cardiac remodeling. *Cardiovasc Res*. 2006; 69:574–584. [PubMed: 16253214]
38. Zitvogel L, Kepp O, Kroemer G. Decoding cell death signals in inflammation and immunity. *Cell*. 2010; 140:798–804. [PubMed: 20303871]
39. Patel VA, Lee DJ, Longacre-Antoni A, Feng L, Lieberthal W, Rauch J, et al. Apoptotic and necrotic cells as sentinels of local tissue stress and inflammation: response pathways initiated in nearby viable cells. *Autoimmunity*. 2009; 42:317–321. [PubMed: 19811288]
40. Wilson NS, Dixit V, Ashkenazi A. Death receptor signal transducers: nodes of coordination in immune signaling networks. *Nat Immunol*. 2009; 10:348–355. [PubMed: 19295631]
41. Kim YS, Morgan MJ, Choksi S, Liu ZG. TNF-induced activation of the Nox1 NADPH oxidase and its role in the induction of necrotic cell death. *Mol Cell*. 2007; 26:675–687. [PubMed: 17560373]
42. Suter PM, Suter S, Girardin E, Roux-Lombard P, Grau GE, Dayer JM. High bronchoalveolar levels of tumor necrosis factor and its inhibitors, interleukin-1, interferon, and elastase, in patients with adult respiratory distress syndrome after trauma, shock, or sepsis. *Am Rev Respir Dis*. 1992; 145:1016–1022. [PubMed: 1586041]

43. Molloy RG, O'Riordain M, Holzheimer R, Nestor M, Collins K, Mannick JA, et al. Mechanism of increased tumor necrosis factor production after thermal injury. Altered sensitivity to PGE2 and immunomodulation with indomethacin. *J Immunol.* 1993; 151:2142–2149. [PubMed: 8345198]
44. Faist E, Storck M, Hultner L, Redl H, Ertel W, Walz A, et al. Functional analysis of monocyte activity through synthesis patterns of proinflammatory cytokines and neopterin in patients in surgical intensive care. *Surgery.* 1992; 112:562–572. [PubMed: 1519173]
45. Baran CP, Zeigler MM, Tridandapani S, Marsh CB. The role of ROS and RNS in regulating life and death of blood monocytes. *Curr Pharm Des.* 2004; 10:855–866. [PubMed: 15032689]
46. Roberts RA, Laskin DL, Smith CV, Robertson FM, Allen EM, Doorn JA, et al. Nitrate and oxidative stress in toxicology and disease. *Toxicol Sci.* 2009; 112:4–16. [PubMed: 19656995]
47. Kasahara Y, Iwai K, Yachie A, Ohta K, Konno A, Seki H, et al. Involvement of reactive oxygen intermediates in spontaneous and CD95 (Fas/APO-1)-mediated apoptosis of neutrophils. *Blood.* 1997; 89:1748–1753. [PubMed: 9057659]
48. Challa S, Chan FK. Going up in flames: necrotic cell injury and inflammatory diseases. *Cell Mol Life Sci.* 2010; 67:3241–3253. [PubMed: 20532807]
49. Lin CC, Anseth KS. Controlling Affinity Binding with Peptide-Functionalized Poly(ethylene glycol) Hydrogels. *Adv Funct Mater.* 2009; 19:2325. [PubMed: 20148198]
50. Seager Danciger J, Lutz M, Hama S, Cruz D, Castrillo A, Lazaro J, et al. Method for large scale isolation, culture and cryopreservation of human monocytes suitable for chemotaxis, cellular adhesion assays, macrophage and dendritic cell differentiation. *J Immunol Methods.* 2004; 288:123–134. [PubMed: 15183091]
51. Wang KK, Posner A, Raser KJ, Buroker-Kilgore M, Nath R, Hajimohammadreza I, et al. Alpha-mercaptopropionic acid derivatives as novel selective calpain inhibitors. *Adv Exp Med Biol.* 1996; 389:95–101. [PubMed: 8860998]
52. Levy DE, Lapiere F, Liang W, Ye W, Lange CW, Li X, et al. Matrix metalloproteinase inhibitors: a structure-activity study. *J Med Chem.* 1998; 41:199–223. [PubMed: 9457244]
53. Krysko DV, Vanden Berghe T, D'Herde K, Vandenabeele P. Apoptosis and necrosis: detection, discrimination and phagocytosis. *Methods.* 2008; 44:205–221. [PubMed: 18314051]
54. Palecek SP, Loftus JC, Ginsberg MH, Lauffenburger DA, Horwitz AF. Integrin-ligand binding properties govern cell migration speed through cell-substratum adhesiveness. *Nature.* 1997; 385:537–540. [PubMed: 9020360]
55. Brooks PC, Stromblad S, Sanders LC, von Schalscha TL, Aimes RT, Stetler-Stevenson WG, et al. Localization of matrix metalloproteinase MMP-2 to the surface of invasive cells by interaction with integrin alpha v beta 3. *Cell.* 1996; 85:683–693. [PubMed: 8646777]
56. Morini M, Mottolose M, Ferrari N, Ghiorzo F, Buglioni S, Mortarini R, et al. The alpha 3 beta 1 integrin is associated with mammary carcinoma cell metastasis, invasion, and gelatinase B (MMP-9) activity. *Int J Cancer.* 2000; 87:336–342. [PubMed: 10897037]
57. Turk BE, Huang LL, Piro ET, Cantley LC. Determination of protease cleavage site motifs using mixture-based oriented peptide libraries. *Nat Biotechnol.* 2001; 19:661–667. [PubMed: 11433279]
58. Shastry S, Tyagi SC. Homocysteine induces metalloproteinase and shedding of beta-1 integrin in microvessel endothelial cells. *J Cell Biochem.* 2004; 93:207–213. [PubMed: 15352177]
59. Vaisar T, Kassim SY, Gomez IG, Green PS, Hargarten S, Gough PJ, et al. MMP-9 sheds the beta2 integrin subunit (CD18) from macrophages. *Mol Cell Proteomics.* 2009; 8:1044–1060. [PubMed: 19116209]
60. Turk BE, Wong TY, Schwarzenbacher R, Jarrell ET, Leppla SH, Collier RJ, et al. The structural basis for substrate and inhibitor selectivity of the anthrax lethal factor. *Nat Struct Mol Biol.* 2004; 11:60–66. [PubMed: 14718924]
61. Chiarugi P, Pani G, Giannoni E, Taddei L, Colavitti R, Raugei G, et al. Reactive oxygen species as essential mediators of cell adhesion: the oxidative inhibition of a FAK tyrosine phosphatase is required for cell adhesion. *J Cell Biol.* 2003; 161:933–944. [PubMed: 12796479]
62. Cristofanon S, Nuccitelli S, D'Alessio M, Dicato M, Diederich M, Ghibelli L. Oxidation-dependent maturation and survival of explanted blood monocytes via Bcl-2 up-regulation. *Biochem Pharmacol.* 2008; 76:1533–1543. [PubMed: 18765235]

63. Fuchs TA, Abed U, Goosmann C, Hurwitz R, Schulze I, Wahn V, et al. Novel cell death program leads to neutrophil extracellular traps. *J Cell Biol.* 2007; 176:231–241. [PubMed: 17210947]
64. Bartneck M, Keul HA, Zwadlo-Klarwasser G, Groll J. Phagocytosis independent extracellular nanoparticle clearance by human immune cells. *Nano Lett.* 2010; 10:59–63. [PubMed: 19994869]
65. Majewska E, Sulowska Z, Baj Z. Spontaneous apoptosis of neutrophils in whole blood and its relation to apoptosis gene proteins. *Scand J Immunol.* 2000; 52:496–501. [PubMed: 11119249]
66. Fadok VA, Bratton DL, Konowal A, Freed PW, Westcott JY, Henson PM. Macrophages that have ingested apoptotic cells in vitro inhibit proinflammatory cytokine production through autocrine/paracrine mechanisms involving TGF-beta, PGE2, and PAF. *J Clin Invest.* 1998; 101:890–898. [PubMed: 9466984]
67. Kono H, Rock KL. How dying cells alert the immune system to danger. *Nat Rev Immunol.* 2008; 8:279–289. [PubMed: 18340345]

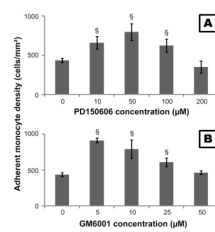


Figure 1.

The number of adherent monocytes on TCPS cultured with various concentrations of (A) PD150606 and (B) GM6001 for 2 hours. Cells without treatment of PD150606 or GM6001 served as the control.

§: significantly different compared to the control at 2 hours, $p < 0.05$.

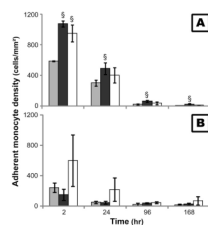


Figure 2. The number of adherent monocytes on TCPS (A) and PEG hydrogel (B) surfaces after 2 hours incubation with 10 μM GM6001 (■) or 50 μM PD150606 (▒) before each time point. Cells cultured without GM6001 or PD150606 served as control (□). §: significantly different compared to the control without additive at the same time point, $p < 0.05$;

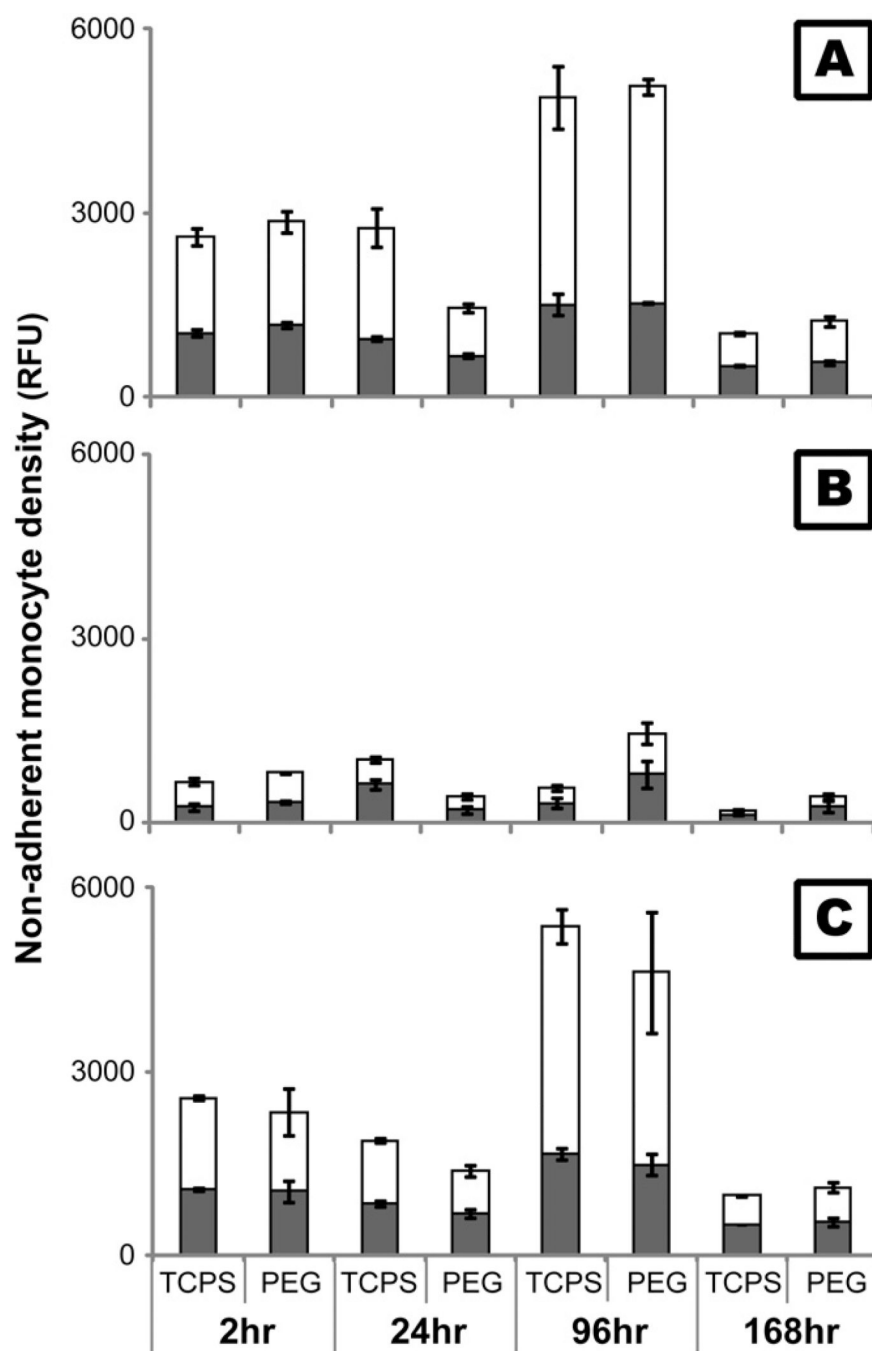


Figure 3. Viable (■) and non-viable (□) monocytes in the cell culture supernatant after treatment with 10µM GM6001 (B) or 50µM PD150606 (C) for 2 hours before each time point on TCPS and PEG hydrogel substrates. The fluorescence of live and dead cells was measured for each sample simultaneously (MultiTox-Fluor™, Promega). Cells cultured on TCPS without GM6001 or PD150606 served as control (A).

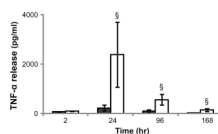


Figure 4.

TNF- α concentration in monocyte culture supernatant on TCPS (■) and PEG hydrogel (□) substrates at 2, 24, 96 and 168 hours.

§: significantly different compared to TCPS at the same time point, $p < 0.05$;

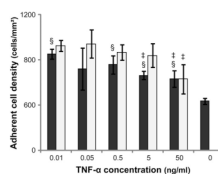


Figure 5.

The adherent monocyte density on TCPS after incubation for 2 (■) or 12 (□) hours in media supplemented 0.01, 0.05, 0.5, 5 or 50 ng/mL human recombinant TNF- α . Media without exogenous TNF- α served as the control.

§: significantly different compared to the control without cells at 2 hours, $p < 0.05$;

‡: significantly different compared to the cell number at the same time point treated with 0.01 ng/mL TNF- α , $p < 0.05$.

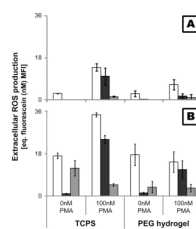


Figure 6. Extracellular ROS production by monocytes (A) and PMNs (B) adhered to TCPS and PEG hydrogels at 2(□), 24(■) and 96(▨) hr. ROS levels were determined using a cell membrane impermeable probe which fluoresces upon oxidation ($485_{ex}/520_{em}$).

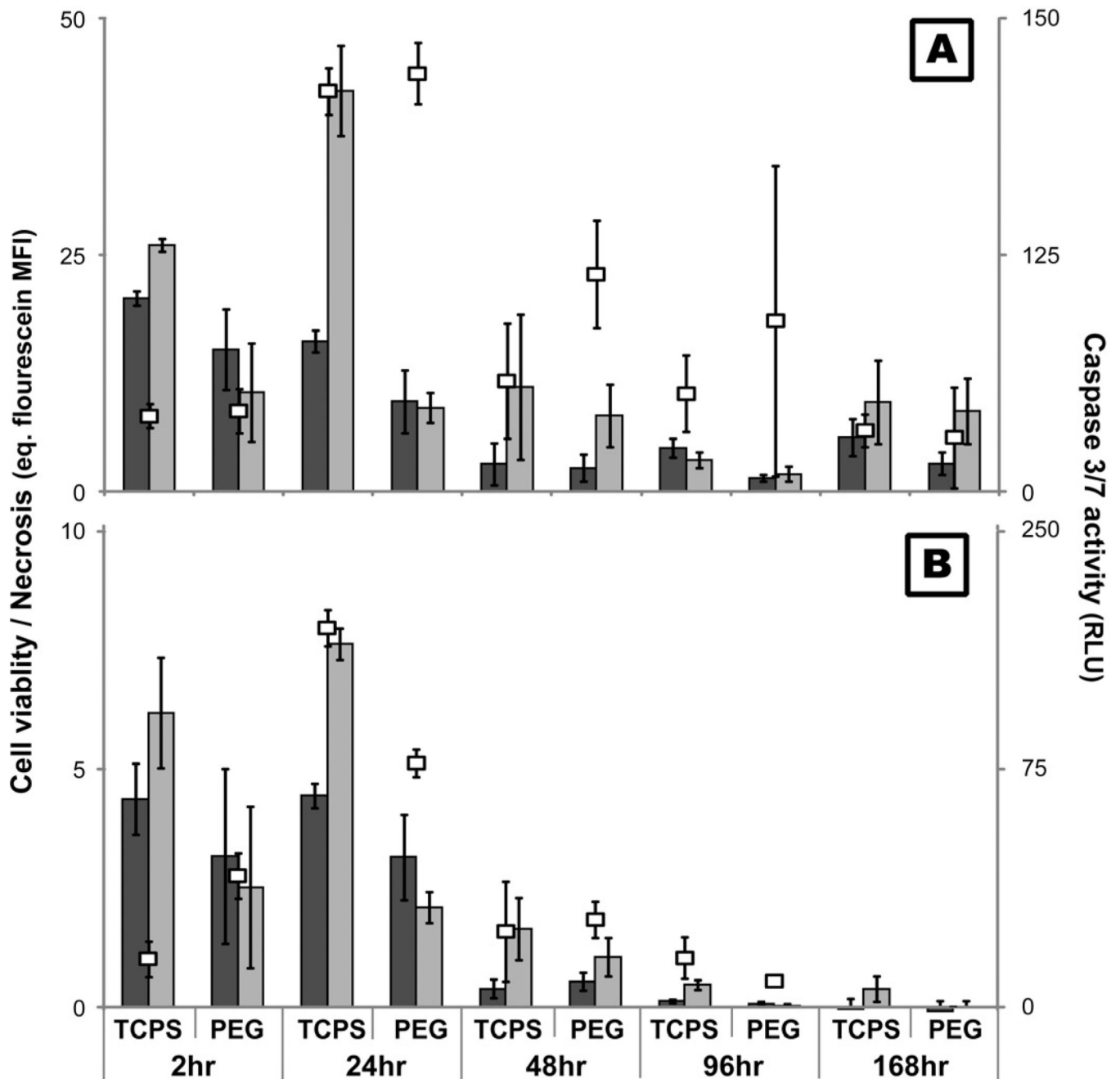


Figure 7.

The level of monocyte (A) and PMN (B) viability (■), apoptosis (□), and necrosis (■) at 2, 24, 48, 96, and 168hr after exposure to TCPS and PEG hydrogel substrates. Viability was assessed by measuring the cleavage of a fluorogenic, cell-permeant, peptide substrate by cells with intact membranes. Primary and secondary necrosis is assessed by measuring the cleavage of fluorogenic, cell-impermeant, peptide substrate, by a “dead-cell protease” which is released from cells with permeable membranes. Mean fluorescent intensity (MFI) of the samples were compared to a fluorescein standard curve to allow for comparison between time points. Finally, cleavage of a luminogenic caspase-3/7 substrate was used to assess apoptosis.

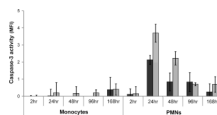


Figure 8. Levels of secondary necrosis present in monocyte and PMN cultures as determined by measuring the activity of caspase-3 in the supernatant. Supernatant from cells exposed to TCPS (■) and PEG hydrogel (□) substrates for 2, 24, 48, 96, and 168hr were exposed to fluorogenic caspase-3 substrate and the mean fluorescence intensity from the cleaved probe was assessed.

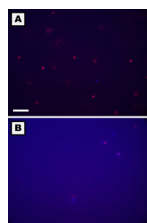


Figure 9. Photomicrographs of apoptotic and necrotic monocytes on TCPS (**A**) and PEG hydrogel (**B**) surfaces at 24hr. Apoptosis detection was based on the translocation of phosphatidylserine from the inner to outer membrane of the plasma membrane in apoptotic cells (**Blue**). Primary and secondary necrosis was detected using the nucleic acid-binding propidium iodide dye which cannot penetrate the membranes of live or early apoptotic cells (**Red**). Live cells demonstrated no or a very low level of fluorescence. The PEG hydrogel created blue background fluorescence. The white reference line represents 75 μ m.